

Separation of current and spin contributions to isovector $M1$ excitations by means of the (e, e') and (p, n) reactions

F. Petrovich

Department of Physics, Florida State University, Tallahassee, Florida 32306

W. G. Love

Department of Physics and Astronomy, University of Georgia, Athens, Georgia 30602

R. J. McCarthy

Department of Physics, Kent State University at Ashtabula, Ashtabula, Ohio 44004

(Received 10 October 1979)

The orbital current and spin contributions to isovector $M1$ excitations in light nuclei are studied microscopically by combining information from inelastic electron scattering at small momentum transfers with that obtained from recent measurements of (p, n) cross sections at forward angles. The (p, n) reaction is studied within the distorted-wave approximation using a G -matrix interaction and shell model wave functions and the (e, e') scattering is calculated in a plane wave approximation.

NUCLEAR REACTIONS Charge exchange scattering, $E_p = 62$ MeV, cross sections; inelastic electron scattering; targets ^{12}C , ^{24}Mg , ^{28}Si .

I. INTRODUCTION

Experimental studies of the (p, n) reaction at $E_p \approx 60$ MeV, currently being carried out at the Indiana University Cyclotron Facility, will provide much new information on isovector modes of excitation in nuclei.¹⁻⁵ In one of the first (p, n) experiments, forward angle cross sections for the excitation of analogs of $1^+ T=1$ levels in ^{12}C , ^{24}Mg , and ^{28}Si by 62 MeV protons were measured. We report here a study of the nature of the isovector dipole transitions in these nuclei based on the shell model wave functions of Cohen and Kurath (^{12}C) (Ref. 6) and Chung and Wildenthal (^{24}Mg , ^{28}Si).⁷ It is shown that a *separate* measure of orbital current and spin transition matrix elements can be obtained by simultaneously considering information from the (p, n) reaction and corresponding information from low momentum transfer inelastic electron scattering.⁸⁻¹¹ The (p, n) reaction is interpreted within the distorted wave approximation and the G -matrix interaction of Bertsch *et al.*¹² is assumed for the effective interaction. The complete spin dependent isovector part of the interaction is compared with the one-pion exchange potential (OPEP) which is expected to be the leading term at small momentum transfer.

II. RELATION BETWEEN THE (e, e') AND (p, n) REACTIONS

For $0^+ \rightarrow J^+$ abnormal parity transitions it is common^{8-11, 13} to characterize the inelastic electron scattering cross sections by the reduced magnetic transition probability. The Born expression for this quantity, which is adequate for the

discussion of electron scattering from light nuclei, is given by¹³

$$B(MJ\uparrow; q) = \left[\frac{(2J+1)!!}{q^{J-1}} \left(\frac{J}{J+1} \right)^{1/2} \frac{e\hbar}{2Mc} \right]^2 \times \left| \sum_{L,t} [C_L^s g_s^t \rho_{JL}^{st}(q) + C_L^i g_i^t \rho_{JL}^{it}(q)] \right|^2, \quad (1)$$

where q is the momentum transfer, L is the orbital angular momentum transfer which is restricted to the values $J-1$ and $J+1$, t differentiates between isoscalar and isovector quantities, g_s^t and g_i^t are the spin and orbital g factors, $C_{J-1}^s = \frac{1}{2}(J+1)^{1/2}$, $C_{J-1}^i = 2(J+1)^{-1/2}$, $C_{J+1}^s = -\frac{1}{2}J^{1/2}$, $C_{J+1}^i = 2J^{-1/2}$, and $\rho_{JL}^{st}(q)$ and $\rho_{JL}^{it}(q)$ are the momentum representations of the spin and orbital current transition densities defined by

$$\rho_{JL}^{kt}(q) = \langle J^+ || \sum_i j_L(qr_i) [Y_L(\hat{r}_i) \times O_i^k] \tau_i^t || 0 \rangle, \quad (2)$$

where $\langle || || \rangle$ denotes a reduced matrix element,¹⁴ $j_L(qr_i)$ is a spherical Bessel function, and O_i^k is $\bar{\sigma}_i$ or \bar{l}_i as k is s or l . We are specifically interested in transitions with $J=t=1$ for which L can be 0 or 2. By expanding the Bessel functions in Eq. (2) about $q=0$ one easily obtains the two parameter formula⁸⁻¹¹ commonly used to describe the low q electron scattering data, i.e.,

$$B(MJ\uparrow; q) = B(MJ\uparrow; 0) \left[1 - \frac{J+3}{J+1} \frac{(qR_{tr})^2}{2(2J+3)} + \dots \right]^2, \quad (3)$$

where $B(MJ\uparrow; 0)$ is the reduced transition probability for γ decay and R_{tr} is the transition radius.

To see the connection between inelastic electron

scattering and the (p, n) reaction for a $0^+ \rightarrow J^\pi$ abnormal parity transition, it is useful to examine the direct microscopic Born approximation expression for the (p, n) cross section. In the case of a local effective interaction with central, tensor, and spin-orbit parts this is¹⁵⁻¹⁷

$$\frac{d\sigma}{d\Omega} = \left(\frac{\mu}{2\pi\hbar^2} \right)^2 \frac{k_f}{k_i} (2J+1) 8\pi \times \left\{ \left| \sum_{L,t} v_i^{LS}(q) B_L^J \rho_{JL}^{st}(q) \right|^2 + \sum_L \left| \sum_t \left[v_i^C(q) \rho_{JL}^{st}(q) + v_i^T(q) \sum_{L'} Z_{LL'}^J \rho_{JL}^{st}(q) + v_i^{LS}(q) A_L^J \rho_{JL}^{st}(q) \right] \right|^2 \right\}, \quad (4)$$

where the factors outside the curly brackets are the usual kinematical and statistical factors, $v^C(q)$, $v^T(q)$, and $v^{LS}(q)$ are the Bessel transforms of the spin-dependent central, tensor, and spin-orbit components of the effective interaction, L' is the orbital angular momentum transfer to the target when the tensor interaction is acting, A_L^J , B_L^J , and $Z_{LL'}^J$ are statistical coefficients which can be obtained elsewhere,¹⁷⁻¹⁹ $\rho_{JL}^{st}(q)$ is the spin transition density, and $\rho_{JL}^{it}(q)$ is a linear combination of the orbital current densities. As in the discussion of Eqs. (1)–(3) we are specifically interested in the case $J=t=1$ for which L and L' can each be either 0 or 2. A proper treatment of the (p, n) reaction requires, of course, the inclusion of distortion effects²⁰ and knockout exchange amplitudes.²¹ These effects are not included explicitly in Eq. (4) because they complicate the relation without affecting its basic sense. Both distortion and knockout exchange are treated *exactly* in the final calculations of the (p, n) cross sections to be discussed below. In the graphs of the effective interaction to be shown, the knockout exchange amplitudes for the central and spin-orbit interaction components are included in the interaction by means of a well established approximation.^{22, 23} At this point, it is clear from Eqs. (1) and (4) that the connection between the (e, e') and (p, n) reactions for $0^+ \rightarrow J^\pi$ abnormal parity transitions is usually complicated.

III. RESULTS

Some of the essential results obtained from the shell model wave functions of Refs. 6 and 7 are summarized in Table I and Fig. 1. The table lists the theoretical and experimental excitation energies, reduced transition probabilities $B(M1\uparrow)$, and transition radii R_{tr} for the first $1^+T=1$ excitation

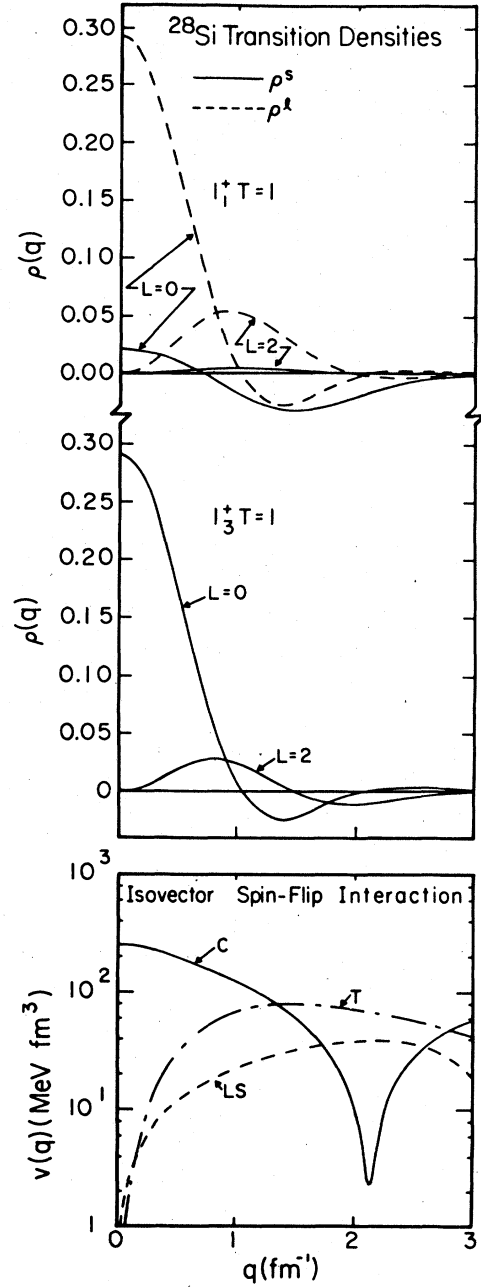


FIG. 1. The $L=0$ and $L=2$ spin and orbital current densities for the 1_1^+ and $1_{3/2}^+$ $T=1$ excitations in ^{28}Si are compared with the isovector spin-flip parts of the G -matrix interaction of Ref. 12. For the $1_{3/2}^+$ $T=1$ excitation the orbital current densities are too small to show in the graph. C , LS , and T refer to the central, spin-orbit, and tensor components of the interaction.

in ^{12}C and the first four $1^+T=1$ levels in ^{24}Mg and ^{28}Si . The last two columns in the table contain the values of the theoretical $L=0$ spin and orbital current transition densities at $q=0$. The complete set ($L=0$ and $L=2$) of theoretical spin and orbital cur-

TABLE I. Comparison of shell model results with experiment for isovector $M1$ transitions in ^{12}C , ^{24}Mg , and ^{28}Si .

Nucleus	Final state	$E_x^{\text{exp } a}$ (MeV)	$E_x^{\text{th } b}$ (MeV)	$B(M1 \uparrow)_{\text{exp } a}$ ($e^2 \text{fm}^2$)	$B(M1 \uparrow)_{\text{th } b}$ ($e^2 \text{fm}^2$)	$R_{\text{tr}}^{\text{exp } a}$ (fm)	$R_{\text{tr}}^{\text{th } b}$ (fm)	$\rho_{10}^{s1}(0)$	$\rho_{10}^{11}(0)$
^{12}C	$1_1^+ T=1$	15.11	15.08	$(3.22 \pm 0.33) \times 10^{-2}$	2.54×10^{-2}	2.70 ± 0.20	2.67	-0.221	0.026
	$1_1^+ T=1$	9.97	10.22	$(1.30 \pm 0.21) \times 10^{-2}$	6.31×10^{-3}	3.05 ± 0.44	3.10	-0.035	-0.339
	$1_2^+ T=1$	10.72	11.14	$(4.10 \pm 0.77) \times 10^{-2}$	3.85×10^{-2}	2.94 ± 0.14	2.94	-0.221	-0.210
^{24}Mg	$1_3^+ T=1$		13.30		3.41×10^{-3}		3.45	-0.156	0.361
	$1_4^+ T=1$		13.59		2.53×10^{-3}		2.75	0.090	-0.104
	$1_1^+ T=1$	10.48	12.05	$(5.99 \pm 2.75) \times 10^{-3}$	3.86×10^{-3}	3.90 ± 0.40	2.78	0.022	0.293
^{28}Si	$1_2^+ T=1$	10.86	12.29	$(1.28 \pm 0.27) \times 10^{-2}$	2.23×10^{-2}	2.98 ± 0.25	2.95	0.186	0.080
	$1_3^+ T=1$	11.41	13.28	$(4.01 \pm 0.77) \times 10^{-2}$	4.64×10^{-2}	2.58 ± 0.23	2.97	-0.292	0.001
	$1_4^+ T=1$	12.27	14.00	$(1.13 \pm 0.29) \times 10^{-2}$	5.26×10^{-3}	2.93 ± 0.36	2.87	-0.098	-0.001

^aReference 11.

^bThe ^{12}C results are from Ref. 6 while the ^{24}Mg and ^{28}Si results are from Ref. 7. Harmonic oscillator radial wave functions were used in the calculations with $b=1.95, 1.82,$ and 1.86 fm for $^{12}\text{C}, ^{24}\text{Mg},$ and ^{28}Si , respectively.

rent transition densities for the 1_1^+ and 1_3^+ $T=1$ excitations in ^{28}Si are shown with the isovector spin-flip components of the G matrix interaction of Ref. 12 in Fig. 1.

From Table I it is clear that the theoretical wave functions give a good qualitative account of the experimental electromagnetic data. One can distinguish between two types of transitions. One type might be called current correlated, i.e., $\rho_{10}^{11} \gg \rho_{10}^{s1}$. The $1_1^+ T=1$ levels in both ^{24}Mg and ^{28}Si are of this type. These are weak in electron scattering because $g_1^1 \approx 0.1g_s^1$. They are weaker still in the (p, n) reaction at low q because ρ_{10}^{11} couples to the projectile through the spin-orbit interaction which is essentially zero at $q=0$. These levels were not seen in the 62 MeV experiment¹⁻⁵ being discussed here. The other type of transition might be called spin dominated, i.e., $g_s^1 \rho_{10}^{s1} > g_1^1 \rho_{10}^{11}$. All of the other excitations in the table fall into this group. The current contributions to the spin dominated states in ^{24}Mg are considerably larger than those for the spin dominated states in ^{12}C and ^{28}Si . This occurs because of the open $j=1d_{5/2}$ shell for ^{24}Mg . It is the $1d_{5/2} \rightarrow 1d_{5/2}$ single particle transition which has the largest current matrix elements in the s - d shell.

Using the fact that the tensor interaction, the spin-orbit interaction, and the $L=2$ transition densities are small near $q=0$, Eqs. (1) and (4) reduce approximately to

$$B(M1 \uparrow; q) \approx g \left(\frac{e\hbar}{2Mc} \right)^2 \left| \frac{1}{2} g_s^1 \rho_{10}^{s1}(q) + g_1^1 \rho_{10}^{11}(q) \right|^2, \quad (5)$$

$$\frac{d\sigma}{d\Omega} \approx 8\pi \left(\frac{\mu}{2\pi\hbar^2} \right)^2 \frac{k_f}{k_i} 3 \left| v_1^C(q) \rho_{10}^{s1}(q) \right|^2 \quad (6)$$

for the spin dominated transitions at low q . These relations clearly show that the scaling of the forward (p, n) cross sections for spin dominated transitions measures the scaling of the $L=0$ spin transition densities at low q and departures in the scaling of $M1$ rates and forward (p, n) cross sections are a direct consequence of the $L=0$ orbital current transition densities at low q .

Equations (5) and (6) do not allow for a model independent determination of $v_1^C(q)$ at low q since there are two experimental values, $B(M1 \uparrow; q)$ and $d\sigma/d\Omega$, and two structure unknowns, ρ_{10}^{s1} and ρ_{10}^{11} , for each transition. β decay is more useful in this regard because allowed Gamow-Teller decays provide a direct measure of $\rho_{10}^{s1}(0)$ (Refs. 24 and 25) which can be used in Eq. (6). The essential relation is

$$\langle \sigma \rangle^2 = 6\pi \left| \rho_{10}^{s1}(0) \right|^2, \quad (7)$$

where $\langle \sigma \rangle^2$ is the Gamow-Teller matrix element. There are no β -decay data available for transitions in ^{24}Mg and ^{28}Si . The $^{12}\text{N}(1^+) \rightarrow ^{12}\text{C}(0^+) \beta^+$ rate^{10,26} implies that $\rho_{10}^{s1}(0) = 0.223$ for the $0^+ \rightarrow 1_1^+ T=1$ transition in ^{12}C . This is quite close to the value of 0.221 obtained from the Cohen and Kurath wave functions so this transition serves to fix $v_1^C(q)$. In addition, it is concluded that the discrepancy between the experimental and theoretical $B(M1 \uparrow)$ for this transition is associated with the orbital current transition density. Multiplication of $\rho_{10}^{11}(0)$ in Table I by about -2 is sufficient to remove the discrepancy.

The results of theoretical distorted wave calculations are compared with the experimental (p, n) data in Fig. 2. The theoretical (p, n) cross sec-

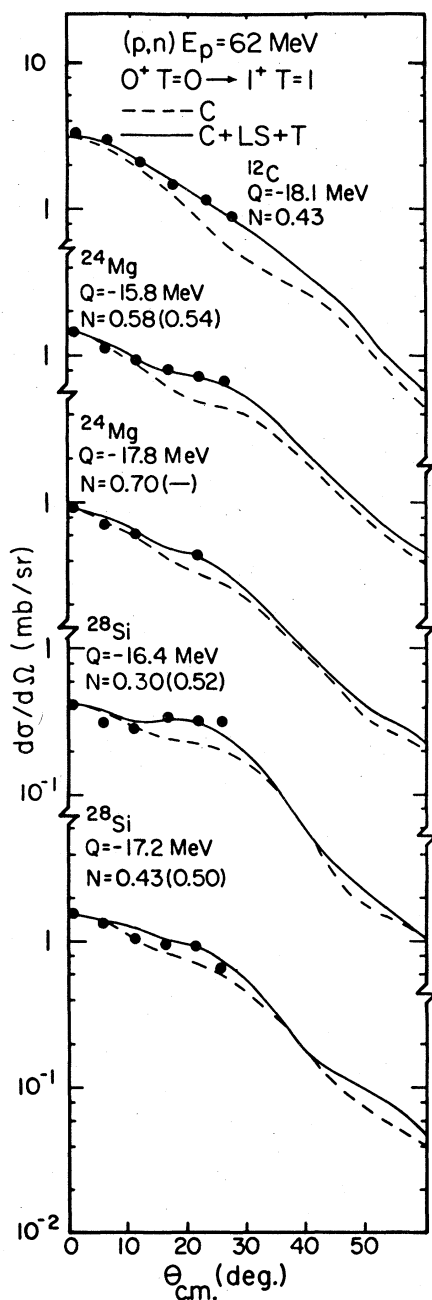


FIG. 2. The results of the distorted wave calculations normalized to the data as described in the text. The dashed curves are the results obtained with the central components of the G -matrix interaction alone and the solid curves are the results obtained with the complete G -matrix interaction. The levels observed in ^{24}Mg and ^{28}Si correspond to the $1\frac{1}{2}^+$ and $1\frac{3}{2}^+$ $T=1$ excitations listed in Table I.

tions have been calculated with the computer code DWBA70 (Ref. 27) using the wave functions of Refs. 6 and 7, the G matrix interaction of Ref. 12, and

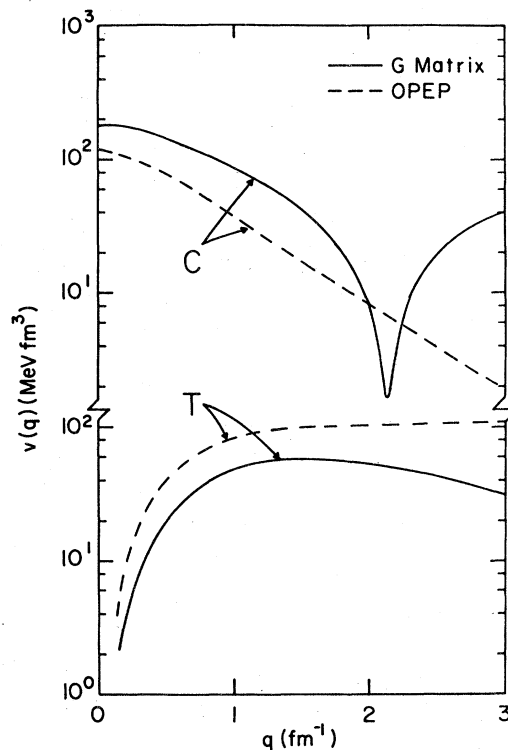


FIG. 3. A comparison of the central and tensor parts of the G -matrix interaction of Ref. 12 (reduced by the factor 1.4) with the corresponding parts of the OPEP.

optical model parameters of Ref. 28. The theoretical results give a good reproduction of the shape of the experimental data, but have to be renormalized by factors $N = 0.3-0.7$ to reproduce the magnitude of the experimental cross sections. The noncentral components of the effective interaction make essentially no contributions to the (p,n) cross sections at 0° . They do enter and improve the shape of the (p,n) cross sections at larger angles. Much less scatter is obtained in the normalization factors if the theoretical wave functions are first normalized to the experimental $B(M1\uparrow)$. This is reflected in the normalization factors shown in parentheses in Fig. 2. This prescription was not applied to the ^{12}C transition because of the β -decay information discussed above. The calculation for the $^{24}\text{Mg}(p,n)$ transition to the analog of the $1\frac{3}{2}^+$ state was not renormalized either since the corresponding transition is not observed in (e,e') . The fact that this transition is seen in the (p,n) reaction but not in (e,e') experiments supports the large cancellation between spin and current terms predicted by the Chung-Wildenthal wave functions. This further emphasizes the complementary information which can be obtained from comparative studies of this type. Excluding the $1\frac{3}{2}^+$ state in ^{24}Mg ,

the final renormalization factors range from $N = 0.43$ to $N = 0.54$. One could attempt to reduce further the discrepancy between the normalization factor for ^{12}C compared to ^{24}Mg and ^{28}Si by making additional adjustments in the spin and orbital current densities for ^{24}Mg and ^{28}Si . Uncertainties in the effects of distortion for the scattering of 62 MeV protons from ^{12}C (Ref. 28) are, however, comparable to the existing discrepancy so this has not been done.

It is concluded from these results that the isovector spin-flip components of the G -matrix interaction of Ref. 12 are too strong by a factor of approximately 1.4 at low q . In keeping with current interest in describing the (p, n) reaction in terms of amplitudes which might be considered elementary,²⁹ the central and tensor components of the G -matrix interaction of Ref. 12 (reduced by 1.4) are compared with the corresponding components of the OPEP in Fig. 3. The corrected G matrix $v_1^C(0)$ is 180 MeV fm³ which is to be compared with the OPEP value of 119 MeV fm³, so that OPEP accounts for approximately 44% of the forward (p, n) cross sections at $E_p = 62$ MeV. The present calculations are currently being extended to the newer experimental (p, n) data for incident energies near 120 MeV.¹⁻⁵ Preliminary results^{15, 16, 30} indicate that the t matrix interaction of Ref. 31 is adequate for describing the forward (p, n) cross sections for isovector $M1$ excitations near 120 MeV. OPEP accounts for about 60% of the forward (p, n) cross sections at this higher energy. These results are only in qualitative agreement with results based on partially conserved axial-vector current (PCAC) and the absorption model.²⁹

IV. SUMMARY

In summary the manner in which experimental data from the (p, n) and (e, e') reactions at low momentum transfers can be used to separate the orbital current and spin contributions to isovector $M1$ transitions has been demonstrated. It was necessary to introduce the available β -decay rate for the single transition in ^{12}C to fix the strength of the effective interaction used in the description of the (p, n) reaction. Specific results are that the wave functions of Cohen and Kurath⁶ give a good description of $\rho_{10}^{s1}(0)$, but not $\rho_{10}^{i1}(0)$, for the $0^+ \rightarrow 1_1^-$ $T = 1$ transition in ^{12}C while the Chung and Wildenthal wave functions⁷ for ^{24}Mg and ^{28}Si give about the correct values for $\rho_{10}^{i1}(0)/\rho_{10}^{s1}(0)$, but miss somewhat on the overall magnitude of these quantities. The large orbital current contributions to the ^{24}Mg transitions is a striking feature of the latter wave functions that is consistent with the data. In addition it has been shown that the isovector spin-flip components of the G -matrix interaction of Ref. 12 are about 40% too strong and that the OPEP accounts for only about 44% of the forward angle (p, n) cross sections at $E_p = 62$ MeV.

ACKNOWLEDGMENTS

We would like to thank the authors of Refs. 1-5 for providing us with their data prior to publication and M. B. Greenfield for help with some of the calculations. Additional thanks go to D. Kurath and B. H. Wildenthal for helpful correspondence concerning their nuclear wave functions. This work was supported in part by the National Science Foundation.

¹B. D. Anderson, D. E. Bainum, A. Baldwin, C. C. Foster, C. D. Goodman, C. A. Goulding, M. B. Greenfield, J. N. Knudson, R. Madey, J. Rapaport, and T. R. Witten, IUCF Technical and Scientific Report 1977-1978 (unpublished), p. 117.

²C. D. Goodman, in *Proceedings of the LAMPF Workshop on Pion Single Charge Exchange, Los Alamos, 1979*, Report No. LA-7892C, p. 23.

³C. D. Goodman, in *The (p, n) Reaction and the Nucleon-Nucleon Force*, edited by C. D. Goodman *et al.* (Plenum, New York, 1980), p. 149.

⁴C. A. Goulding, M. B. Greenfield, C. C. Foster, T. E. Ward, J. Rapaport, D. E. Bainum, and C. D. Goodman, Nucl. Phys. **A331**, 29 (1979).

⁵B. Anderson, D. Bainum, A. Baldwin, C. C. Foster, A. I. Galonsky, C. D. Goodman, C. Goulding, D. Horen, J. Knudson, D. Lind, R. Madey, J. Rapaport, G. R. Satchler, S. D. Schery, G. Walker, J. Watson, T. Witten, and C. Zafiratos, IUCF Technical and Scientific Report 1978 (unpublished), p. 45.

⁶S. Cohen and D. Kurath, Nucl. Phys. **73**, 1 (1965); **A101**, 1 (1976); D. Kurath, private communication.

⁷B. H. Wildenthal, in *The (p, n) Reaction and Nucleon-Nucleon Force*, edited by C. D. Goodman *et al.* (Plenum, New York, 1980), p. 89; W. Chung and B. H. Wildenthal (unpublished).

⁸L. W. Fagg, W. L. Bendel, R. A. Tobin, and H. T. Kaiser, Phys. Rev. **171**, 1250 (1968).

⁹L. W. Fagg, W. L. Bendel, E. C. Jones, Jr., and S. Numrich, Phys. Rev. **187**, 1378 (1969).

¹⁰B. T. Chertok, C. Sheffield, J. W. Lightbody, Jr., S. Penner, and D. Blum, Phys. Rev. **C 8**, 23 (1973).

¹¹H. Theissen, *Springer Tracts in Modern Physics*, Vol. **65** (Springer, Berlin, 1972), p. 1.

¹²G. Bertsch, J. Borysowicz, H. McManus, and W. G. Love, Nucl. Phys. **A284**, 399 (1977).

¹³T. de Forest, Jr. and J. D. Walecka, Adv. Phys. **15**, 1 (1966).

¹⁴D. M. Brink and G. R. Satchler, *Angular Momentum* (Oxford University Press, Oxford, 1962).

- ¹⁵F. Petrovich and W. G. Love, in *Proceedings of the LAMPF Workshop on Pion Single Charge Exchange, Los Alamos, 1979*, Report No. LA-7892C, addendum.
- ¹⁶F. Petrovich, in *The (p, n) Reaction and the Nucleon-Nucleon Force*, edited by C. D. Goodman *et al.* (Plenum, New York, 1980), p. 115.
- ¹⁷F. Petrovich and W. G. Love (unpublished).
- ¹⁸W. G. Love and L. J. Parish, Nucl. Phys. A157, 625 (1970).
- ¹⁹W. G. Love, Nucl. Phys. A192, 49 (1972).
- ²⁰G. R. Satchler, Nucl. Phys. 55, 1 (1964).
- ²¹K. A. Amos, V. A. Madsen, and I. E. McCarthy, Nucl. Phys. A94, 103 (1967).
- ²²F. Petrovich, H. McManus, V. A. Madsen, and J. Atkinson, Phys. Rev. Lett. 22, 895 (1969).
- ²³W. G. Love, Nucl. Phys. A312, 160 (1978).
- ²⁴J. D. Anderson, C. Wong, and V. A. Madsen, Phys. Rev. Lett. 24, 1074 (1970).
- ²⁵A. Bohr and B. Mottelson, *Nuclear Structure* (Benjamin, New York, 1969, Vol. I, p. 345).
- ²⁶F. Ajzenberg-Selove, Nucl. Phys. A248, 1 (1975).
- ²⁷J. Raynal and R. Schaeffer, computer code DWBA70.
- ²⁸C. B. Fulmer, J. B. Ball, A. Scott, and M. L. Whiten, Phys. Rev. 181, 1565 (1969).
- ²⁹G. L. Moake, L. J. Gutay, R. P. Scharenberg, P. T. Debevec, and P. A. Quin, Phys. Rev. Lett. 43, 910 (1979); G. L. Moake, L. J. Gutay, R. P. Scharenberg, P. T. Debevec, and P. A. Quin (unpublished).
- ³⁰W. G. Love, in *The (p, n) Reaction and the Nucleon-Nucleon Force*, edited by C. D. Goodman *et al.* (Plenum, New York, 1980), p. 23.
- ³¹W. G. Love, A. Scott, F. Todd Baker, W. P. Jones, and J. D. Wiggins, Jr., Phys. Lett. 73B, 277 (1978).